Newly-Designed Complex Ternary Pt/PdCu Nanoboxes Anchored on Three-Dimensional Graphene Framework for Highly Efficient Ethanol Oxidation

*Chuangang Hu, Huhu Cheng, Yang Zhao, Yue Hu, Yong Liu, Liming Dai, and Liangti Qu**

Fuel cells powered by hydrogen or small organic molecules are environment-friendly and have high energy conversion efficiency, low emissions, and simplicity in device fabrication.[1] Ethanol, with its high energy density, low toxicity, large scale of production from renewable sources, and easy storage and transportation, is one of the ideal combustible materials for fuel cells. However, commercialization of direct ethanol fuel cells has been obstructed by the low-efficiency oxidation of ethanol at the existing electrocatalysts.[2–4] The development of highly active catalysts for oxidation of fuel molecules is one of the vital needs for practical applications of fuel cell devices. Due to the low activity of non-noble catalysts, considerable efforts have been devoted to the optimization of the existing platinum (Pt) nanoparticle catalysts and to the design of new catalyst systems with less usage of Pt as anode catalysts for direct fuel cells.[2,5,6] Pt loading can be decreased by reducing their size for enhanced specific surface areas per mass or using high surface area supporting materials.[7] Recent research has focused on the fabrication of multicomponent metal catalysts to modify the Pt electronic structure and improve the Pt catalytic efficiency.[2] Indeed, the combination of non-noble metals with Pt has provided an effective pathway to reduce the overall use of expensive Pt and the risk of poisoning.[2,8] In particular, ternary electrocatalysts have shown superb electrocatalytic activity in many aspects toward fuel oxidation superior to their binary counterparts,[9,10] and hold the great promise for resolving the aforementioned challenges to develop direct ethanol fuel cells (DEFCs) of practical significance.[10] Apart from the composition, the geometry of catalysts directly associated with the surface atomic arrangement must also be precisely controlled for high-efficiency active electrocatalysis. For example, hollow nanostructures favor high catalytic performance and utilization efficiency because of their lower densities and higher surface areas.[11] As a representative of geometry-defined Pt-based catalysts, Pt nanocubes have received significant attention due to their superior electrocatalytic activity.[12–14] However, to the best of our knowledge, there have been no report on the preparation of ternary Pt-based nanocubes in either hollow or solid state, and thus their electrocatalytic behavior remains unknown so far.

Graphene is an attractive supporting material for catalyst loading owing to its fast 2D electron-transfer kinetics, large surface areas, high mechanical, thermal and chemical stability.[15,16] On the other hand, the abundant functional groups on the surfaces of graphene oxide precursor provide many favorable sites for anchoring the functional nanocomponents, such as catalyst nanoparticles.[17,18] However, the strong planar stacking of 2D graphene sheets by forming irreversible agglomerates[19,20] leads to a drastic loss of electroactive sites during the electrode assembly. As a consequence, 3D porous graphene structure[21,22] is highly desirable for catalyst loading to facilitate the mass transfer and maximize the accessibility to the catalyst surfaces.

We have recently fabricated the graphene-based cathodic catalysts for fuel cell applications.[23–25] Herein, we develop the shape-defined ternary Pt/PdCu nanoboxes anchored onto 3D graphene framework (3DGF) as a new complex catalyst system for anodic electrocatalysis. The shape-defined ternary Pt/PdCu on 3DGF catalyst system is desinged on the basis of the following considerations: (i) Pd and Cu are less expensive and widespread in the earth. (ii) Hollow PdCu binary alloy cubes are available via a solvothermal approach.[26] (iii) Pd has extemely high lattice match with Pt,[27,28] and the obtained PdCu binary has the same face-centered cubic (fcc) structure like Pt, favoring the deposition of Pt for the formation of a ternary structure and the creation of a high activity in catalytic process. (iv) Cu could induce the Pt formation by galvanic displacement reaction.[29,30] (v) PdCu alloy itself is electrochemically active for ethanol oxidation reaction[31] and synergetic effects on electrocatalysis are expected for PdCu and Pt. (vi) 3D graphene framework can be obtained by hydrothermal treatment of graphene oxide,[32] which should be compatible with the solvothermal approach to PdCu binary alloy cubes mentioned above. (vii) 3D porous graphene structure as a support for Pt/PdCu will provide the maximum

C. Hu, H. Cheng, Y. Zhao, Y. Hu, Prof. L. Qu
Key Laboratory of Cluster Science
Ministry of Education of China
School of Chemistry
Beijing Institute of Technology
Beijing 100081, P. R. China
E-mail: lqu@bit.edu.cn

Prof. Y. Liu
Institute of Advanced Materials for Nano-Bio Applications
School of Ophthalmology and Optometry
Wenzhou Medical College
Wenzhou, Zhejiang 325027, P. R. China

Prof. L. Dai
Department of Macromolecular Science and Engineering
Case School of Engineering
Case Western Reserve University
10900 Euclid Avenue, Cleveland, Ohio 44106, United States

DOI: 10.1002/adma.201200498

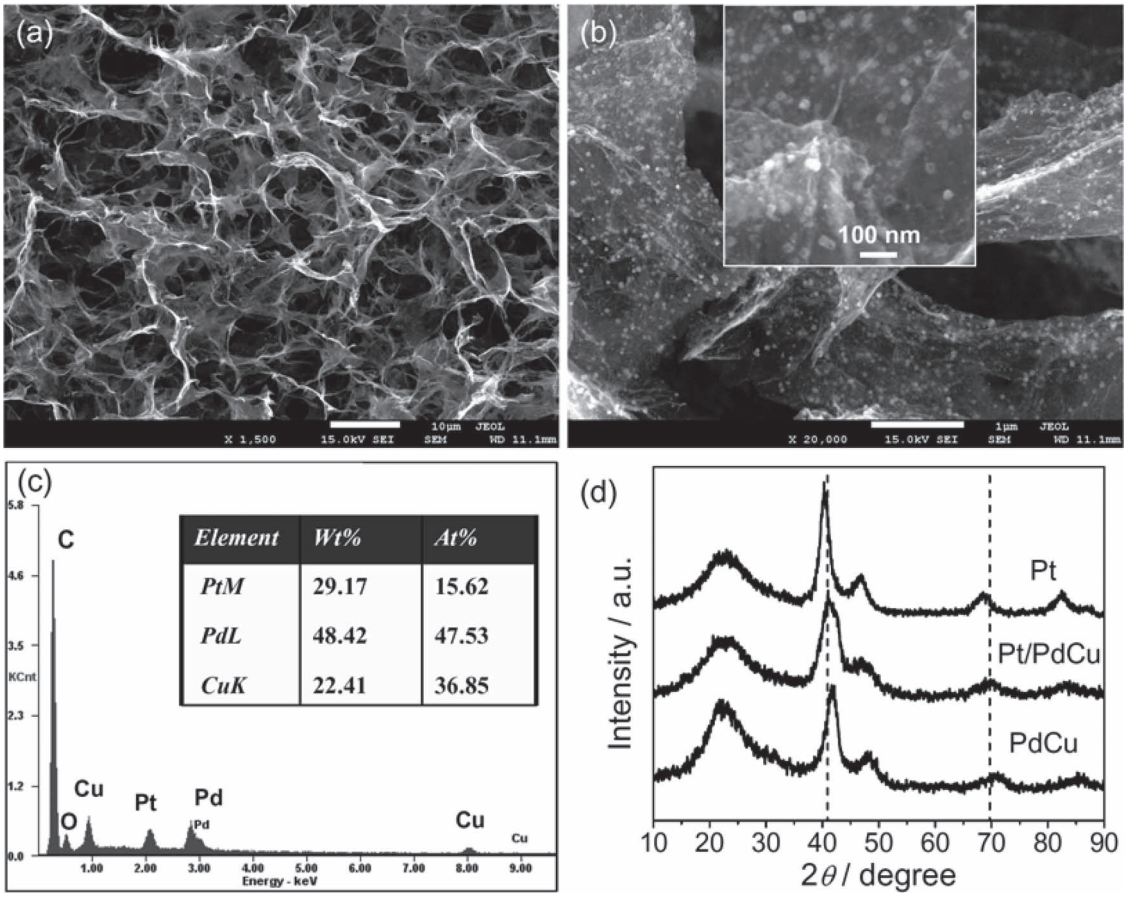

Figure 1. (a,b) FE-SEM images of the Pt/PdCu on 3DGF, (c) the corresponding EDS spectroscopy, and (d) XRD patterns of Pt, PdCu, and Pt/PdCu on 3DGF. The inset in (b) is a high magnification view of cubic Pt/PdCu on graphene sheets.

accessibility for active species to the catalysts to ensure an effective mass transfer of reactants and/or products.[33,34]

To achieve this goal, we have devised a dual solvothermal process to prepare the ternary Pt/PdCu hollow nanocubes on 3DGF. Briefly, we first developed a facile one-pot solvothermal strategy to fabricate the 3DGF with in-situ formed hollow binary PdCu nanocubes. Palladium(II) and copper(II) salts with a 1:1 atomic ratio, glutamate, and graphene oxide were simultaneously added into ethylene glycol (EG) in a stainless-steel autoclave, which was then heated at 160 °C for 7 h to prepare the hollow alloyed nanocubes on porous graphene structure. This solvothermal approach worked well for the formation of 3D graphene framework similar to those synthesized hydrothermally (Figure S1).[32] Hollow PdCu nanocubes[26] were uniformly anchored onto the graphene sheets (Figures S2 and S3), and the formation of alloyed PdCu was confirmed by the XRD pattern in Figure S4. The ternary Pt/PdCu nanoboxes were subsequently formed by reducing H_2PtCl_6 with EG in the presence of glutamate and depositing Pt on the cubic PdCu through the second solvothermal process. EG will effective reduce Pt ions (Table S1) and the existence of glutamate will lead to the selective deposition of Pt on PdCu particles (Figure S5).

The formed ternary Pt/PdCu nanocubes on 3DGF are shown in **Figure 1**. The field-emission scanning electron microscopic (FE-SEM) image exhibits a well-defined and interconnected 3D porous network of graphene sheets (Figure 1a), consistent with the hydrothermally synthesized 3D graphene.[32] Pt/PdCu nanocubes covered all around the individual graphene sheets with a uniform size of *ca.* 30 nm (Figure 1b). The energy dispersive spectroscopy (EDS) (Figure 1c) reveals that the sample is mainly composed of C, Pd, Pt and Cu elements plus O associated with the hydrothermally reduced graphene oxide.[30] The atomic ratio of Pt, Pd and Cu in the nanocubes is *ca.* 0.33/1.0/0.78, which is approximate to the stoichiometric proportion of initial reactants and matchs well with the analysis of inductively coupled plasma-mass spectrometry (ICP-MS). The Pd:Cu atomic ratio in Pt/PdCu nanocubes is slightly higher than that of the initial PdCu nanocubes (1/1.1) (Figure S2,d), indicating that partial displacement reaction, similar to our previous report,[29,30] probably occurred between Cu and H_2PtCl_6 during the formation of ternary Pt/PdCu nanocubes (Table S1). The mass ratio of C, Pt, Pd and Cu comfirmed by ICP-MS analysis is 75.32%, 5.81%, 12.95%, 5.92%.

X-ray diffraction (XRD) pattern of the Pt/PdCu on 3DGF further verified the composition profile in comparison with Pt and PdCu on 3DGF synthesized under the same conditions (Figure 1d). The broad peak located at $2\theta \approx 23°$ is assigned to the (002) plane of stacked graphene sheets within 3DGF.[32] The PdCu

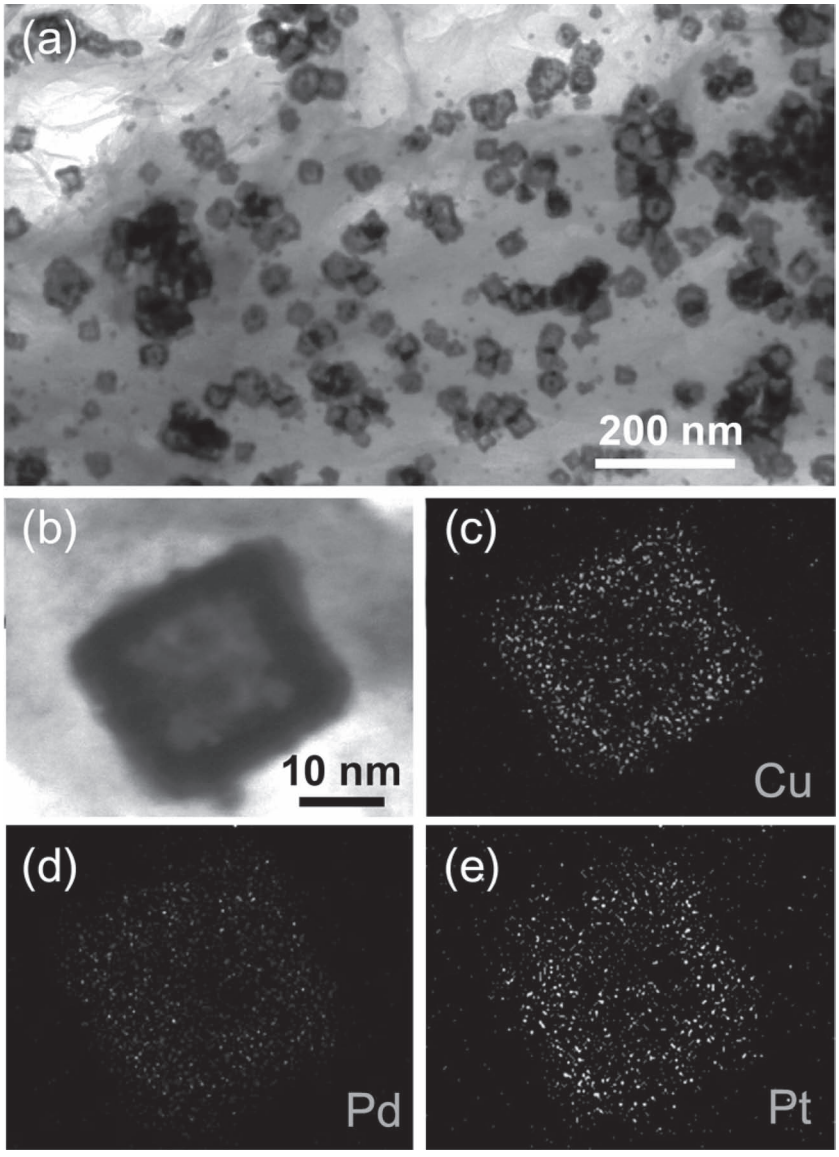

Figure 2. (a) TEM images of Pt/PdCu nanocubes on graphene sheets, (b) HAADF-STEM image of a hollow Pt/PdCu nanocube, (c–e) HAADF-STEM-EDS mapping images of Cu, Pd, and Pt elements, respectively.

and Pt on graphene sheets have characteristic peaks of face-center cubic crystals (Figure 1d).[26,35] Accordingly, the ternary Pt/PdCu nanocubes present typical diffraction peaks similar to those of PdCu and Pt, while the main peaks of Pt/PdCu shift to the transitive diffraction angles corresponding to those of PdCu and Pt, suggesting that Pt has been effectively intercalated into the PdCu domains.

The formation of hollow Pt/PdCu nanocubes was confirmed by the transmission electron microscopy (TEM) images in **Figure 2**a and b. Even after the ultrasonication for preparation of TEM sample, the Pt/PdCu nanocubes are still firmly anchored onto the graphene sheets (Figure 2a). Figure 2b shows a high angle annular dark field scanning transmission electron microscopy (HAADF-STEM) image of a single hollow nanocube with a size of *ca.* 30 nm, exhibiting an internal cavity with a uniform shell of *ca.* 5 nm. The elemental mappings reveal that Cu, Pd, and Pt elements are coexistently distributed along the nanobox shells, and Pt is mixed with PdCu, which is also verified by STEM-EDS line scaning (Figure S6) and X-ray photoelectron spectroscopy (Figure S7), evidencing the formation of ternary Pt/PdCu hollow nanocubes. Accordingly, HR-TEM image further reveals the coexistence of lattice spacings of 0.21 nm and 0.23 nm in the Pt/PdCu nanocube (Figure S8), corresponding to the (111) interplanar distance of face-centered cubic PdCu alloy[26] and a standard Pt crystalline lattice,[36] respectively. These results show the hybrid structure of Pt and PdCu within the hollow nanocubes.

To evaluate the catalytic activity of ternary Pt/PdCu nanoboxes on 3DGF, we investigated the electrooxidation reaction of ethanol in basic medium. **Figure 3**a shows the cyclic voltammograms (CVs) of ethanol oxidation in a 1.0 M KOH + 1.0 M C_2H_5OH solution at a scan rate of 50 mV s^{-1} on Pt/3DGF (Pt loading: 0.032 mg cm^{-2}), PdCu/3DGF (Pd loading: 0.057 mg cm^{-2}), Pt/PdCu/3DGF (Pt loading: 0.020 mg cm^{-2} + Pd loading:0.042 mg cm^{-2}), and 20% Pt/C (Pt loading: 0.069 mg cm^{-2}) electrodes. The metal contents were evaluated by ICP-MS analysis. The onset potential for the ethanol oxidation on the Pt/PdCu/3DGF electrode is *ca.* –0.6 V, which is 100 mV more negative than the *ca.* –0.5 V observed on Pt/3DGF electrode, PdCu/3DGF electrode and the commercial 20% Pt/C electrocatalysts (Figure S9). The reduction in the onset anodic potential shows the significant enhancement in the kinetics of the ethanol oxidation reaction. Ethanol oxidation is characterized by well-separated anodic peaks in the forward and reverse scans. Thus, the magnitude of the anodic peak current density (*j*) in the forward scan is also directly proportional to the amount of ethanol oxidized at the catalyst electrodes.[37,38] The peak current density is 183 mA cm^{-2} for the reaction on Pt/PdCu/3DGF electrode, which is more than 3, 4, and 6 times those on the 20% Pt/C electrode (55 mA cm^{-2}), Pt/3DGF electrode (45 mA cm^{-2}) and PdCu/3DGF electrode (27 mA cm^{-2}), respectively. A more than 6-fold improvement in activity per unit mass of Pt over the commercial Pt/C catalyst (E-TEK 20%) was obtained for the Pt/PdCu/3DGF electrode based on the peak current density. We have also evaluated the activity of Pt/PdCu/3DGF on the basis of the total mass of active metals. As shown in Figure S10, Pt/PdCu/3DGF owns the highest activity compared with all the other catalysts as normalized to the total mass of available Pt and Pd. An about 4-fold improvement in catalytic activity per unit mass of Pt + Pd for ethanol oxidation over the commercial Pt/C catalyst was observed. The significantly negative

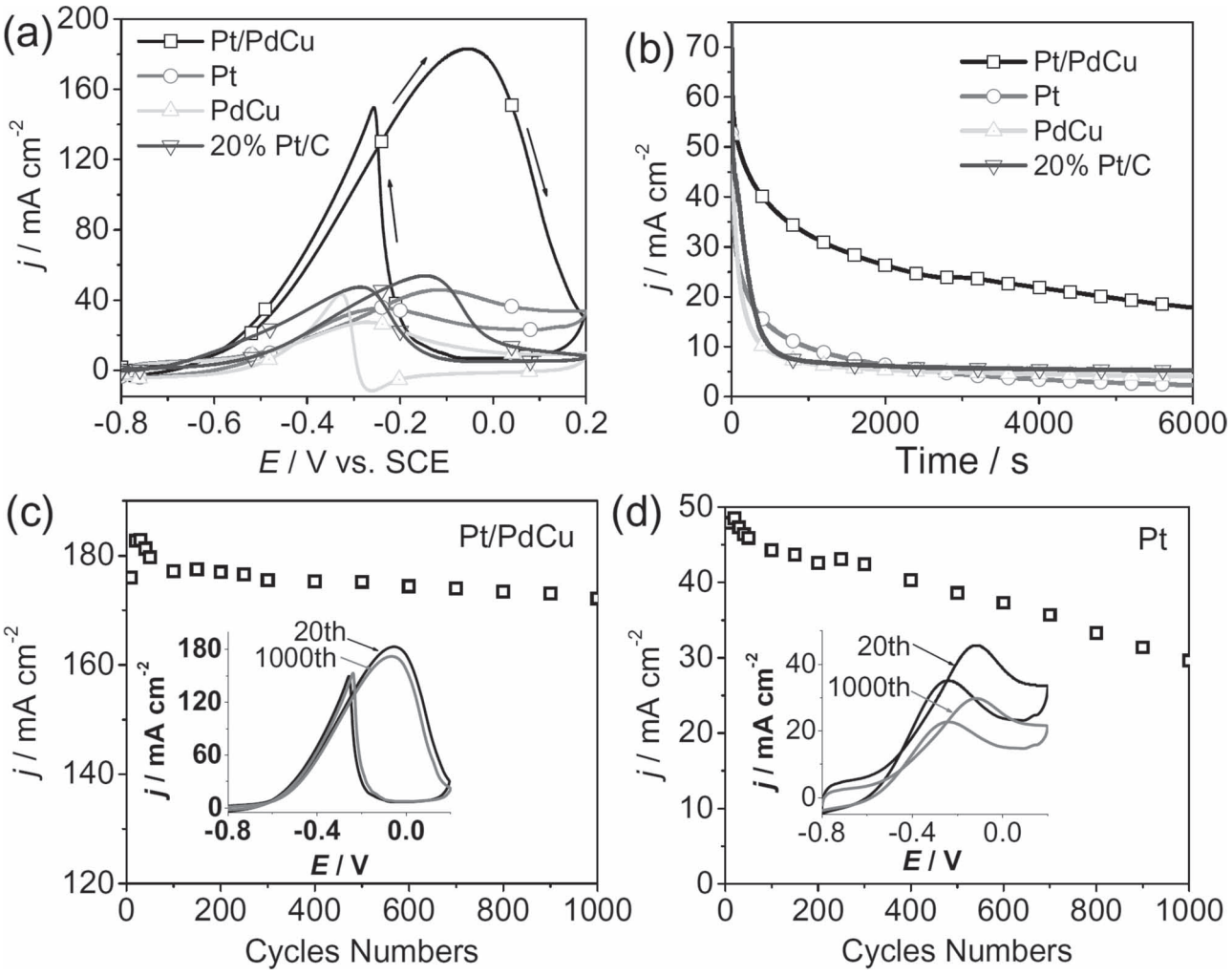

Figure 3. (a) CVs of the Pt/PdCu, Pt, PdCu on 3DGF, and commercial 20% Pt/C catalysts in 1 M CH_3CH_2OH + 1 M KOH aqueous solution. (b) The chronoamperometric curves of the Pt/PdCu, Pt, PdCu on 3DGF, and 20% Pt/C electrodes in 1 M CH_3CH_2OH + 1 M KOH aqueous solution at a given potential of –0.3 V. (c, d) Forward peak current density (*j*) as a function of potential scanning cycles of Pt/PdCu and Pt on 3DGF between –0.8 and 0.2 V in 1 M CH_3CH_2OH + 1 M KOH electrolyte, respectively. The insets in (c) and (d) are the corresponding 20th and 1000th CV curves of Pt/PdCu and Pt on 3DGF. The scan rate: 50 mV s^{-1}.

shift of the onset potential and high anodic peak current for the ethanol electrooxidation reaction on the Pt/PdCu/3DGF electrode illustrate the Pt/PdCu/3DGF electrode has superb electrocatalytic activity for direct ethanol fuel cells. The ternary Pt/PdCu nanocubes on the 3DGF electrocatalyst exhibit a considerably higher activity for ethanol oxidation than that of their Pt and PdCu countparts, highlighting the important synergetic functions of individual components in the ternary system. Although the detailed electrocatalytic oxidation mechanism is still unclear,[2,38] our preliminary results suggested that the oxide species adsorbed on the Pt/PdCu surface could easily desorbe to refresh the active sites and the poison of Pt active sites might have been largely impaired due to the existence of more oxophilic PdCu (Figure S11). Product analysis reveals that both of acetaldehyde and acetic acid exist after electrooxidation of ethanol, indicating the ethanol is oxidized by a mixed 2e and 4e paths (Figure S12).

The electrochemical stability of Pt, PdCu, Pt/PdCu nanoparticles on 3DGF, and 20% Pt/C electrodes for ethanol electrooxidation was investigated by chronoamperometric experiments at a given potential of –0.3 V in 1.0 M KOH + 1.0 M C_2H_5OH solution (Figure 3b). The polarization current for the ethanol electrooxidation reaction shows a rapid decay in the initial period for all the samples, probably due to the formation of the intermediate species during the ethanol electrooxidation reaction in alkaline media. Breaking the C–C bond for a total oxidation to CO_2 is a major problem in ethanol electrocatalysis.[2,38–40] Nevertheless, the Pt/PdCu/3DGF catalyst has much higher anodic current, and the current decay for the reaction on the Pt/PdCu/3DGF electrode is significantly slower than those on the Pt/3DGF, PdCu/3DGF, and 20% Pt/C electrocatalysts. At the end of the 6000 s test, the oxidation current on the Pt/PdCu/3DGF electrode is still 4 times higher than that on all the other electrodes. These results show that the ternary Pt/PdCu

nanoboxes on 3DGF have long-term high catalytic activity for the ethanol electrooxidation reaction in alkaline media.

The high catalytic activity and stability of the Pt/PdCu/3DGF electrode was also demonstrated in Figure 3c in comparsion with single-phase Pt on 3DGF electrode (Figure 3d). The Pt particle size is controlled to be *ca*. 2–3 nm (Figure S13,c), similar to the size of Pt domains within Pt/PdCu cubes. Potential scanning between –0.8 and 0.2 V was carried out for 1000 cycles in 1.0 M KOH + 1.0 M C_2H_5OH solution with a sweep rate of 50 mV s^{-1}. Using the steady state peak current density of the 20th cycle in the forward direction as the reference, the anodic peak current density on Pt/PdCu/3DGF electrode remains about 94% after 1000 cycles (Figure 3c). However, the peak current density of the 1000th cycle on Pt/3DGF electrode is only *ca*. 65% of that measured at the 20th cycle (Figure 3d). The CVs at the 1000th cycle for Pt/PdCu/3DGF is farily similar to the initial one (Figure 3c, inset), while the CVs for Pt/3DGF electrode has been largely compressed (Figure 3d, inset).

In accordance with the durable CV response, the 3D structure of graphene sheets and hollow Pt/PdCu nanocubes present the negligible changes in both morphology and composition after the long-time electrochemical test (Figures S13 and S14). However, drastic agglomeration of pure phase Pt nanoparticles appears after the potential cycling (Figure S13 c and d) most likely due to the Ostwald ripening process.[41] Pt is in general chemically inert and becomes unstable when exposed to the hostile electrochemical environments where Pt surface atoms migrate and agglomerate, resulting in aggregation of nanoparticles and loss of surface area and activity.[41,42] In particular, the instability of Pt at the anode side represents one of the major limitations for commercialization of this technology. The multicomponent Pt/PdCu hollow nanocubes have effectively avoided the aggregation of Pt and remain the high catalytic activity for ethanol oxidation. To investigate the effect of particle size on the catalytic performance, we have also prepared the Pt/3DGF with a Pt size (*ca*. 20–30 nm) close to that of Pt/PdCu nanoboxes (Figure S15). Both the catalytic activity and stablity of Pt/PdCu are much higher than that of Pt with a similar size (Figure S16). On the other hand, besides the synergetic function between Pt and PdCu, our controlled experiments demonstrated that both the advantageous feature of hollow nanocubes and the unique 3D graphene structure as support for catalyst loading play essential roles in enhancing the catalytic performance (Figures S17–S21).

We further fabricate a single cell to demonstrate the potential of the newly-designed Pt/PdCu/3DGF for DEFC application. Despite of the absence of optimization for the experimental conditions and device fabrication in this preliminary study, the alkaline DEFC with a Pt/PdCu/3DGF catalyat gives better performance than that of 20% E-TEK Pt/C in terms of both open-circuit voltage (Voc) and power density (Figure S22). The maximum power density for Pt/PdCu/3DGF is 40 mW cm^{-2}, almost two times that of Pt/C (21 mW cm^{-2}). These results display the potential of Pt/PdCu/3DGF as a good catalyst candidate for commercializing DEFCs.

In summary, we have designed a new complex catalyst system of ternary Pt/PdCu nanoboxes anchored onto 3D graphene sheets by a dual solvothermal process. The electrocatalytic activity of the Pt/PdCu/3DGF for ethanol oxidation are not only significantly higher than that of pure Pt and PdCu electrodes, but also has an about 4-fold improvement over the well-established commercial Pt/C catalysts (E-TEK 20% Pt/C) as normalized to the total mass of active metals, which, in combination with the demonstrated single cell, shows the great potential of the geometry-defined Pt/PdCu/3DGF as excellent electrocatalysts for ethanol electrooxidation in alkaline media for direct ethanol fuel cells.

Experimental Section

The ternary Pt/PdCu hollow nanocubes on 3DGF were prepared by a dual solvothermal process. The aqueous solutions of $PdCl_2$ (6.7 mg/mL, 1.5 mL), GO (8 mg/mL, 3.2 mL), $CuSO_4{\cdot}5H_2O$ (15 mg), and glutamate (50 mg) were mixed together in 40 mL of ethylene glycol (EG). The pH value was adjusted to *ca*. 13 by adding 8 wt% KOH/EG solution. The suspension was then transferred into Teflon-lined stainless-steel autoclave and heated at 160 °C for 7 h. A hydrogel of hollow PdCu nanocubes on 3DGF was obtained, which was then exposed to the EG solution containing appropriate amounts of $H_2PtCl_6{\cdot}6H_2O$ (3.0 mg/mL, 0.9 mL) and 20 mg of glutamate and heated at 160 °C for another 3 h for formation of ternary Pt/PdCu hollow nanocubes on 3DGF. More experimental details and characterization are included in Supporting Information.

Supporting Information

Supporting Information is available from the Wiley Online Library or from the author.

Acknowledgements

This work was supported by NSFC (21004006, 21174019 and 51161120361), 973 program (2011CB013000), the 111 Project B07012, the Ministry of Science and Technology of China (2009DFB30380), the Zhejiang Department of Science and Technology (2009C13019), the Ministry of Education of China (211069), the National "Thousand Talents Program", and the Zhejiang Department of Education (Y200906587). We thank Prof. Yulin Deng for his kind assistance for GC-MS measurement.

Received: February 4, 2012
Revised: April 6, 2012
Published online: August 10, 2012

[1] H. Liu, C. Song, L. Zhang, J. Zhang, H. Wang, P. Wilkinson, *J. Power Sources* **2006**, *155*, 95.
[2] A. Chen, P. Holt-Hindle, *Chem. Rev.* **2010**, *110*, 3767.
[3] J. Mann, N. Yao, A. Bocarsly, *Langmuir* **2006**, *22*, 10432.
[4] S. Sun, M. Chojak Halseid, M. Heinen, Z. Jusys, R. Behm, *J. Power Sources* **2009**, *190*, 2.
[5] Z. Zhou, Z. Huang, D. Chen, Q. Wang, N. Tian, S. Sun, *Angew. Chem. Int. Edt.* **2010**, *49*, 411.
[6] A. Kloke, F. von Stetten, R. Zengerle, S. Kerzenmacher, *Adv. Mater.* **2011**, *23*, 4976.
[7] K. Mayrhofer, V. Juhart, K. Hartl, M. Hanzlik, M. Arenz, *Angew. Chem. Int. Edt.* **2009**, *48*, 3529.
[8] V. Stamenkovic, B. Mun, M. A renz, K. Mayrhofer, C. Lucas, G. Wang, P. Ross, N. Markovic, *Nat. Mater.* **2007**, *6*, 241.
[9] M. Soszko, M. Łukaszewski, Z. Mianowska, A. Czerwiński, *J. Power Sources* **2011**, *196*, 3513.

[10] A. Kowal, M. Li, M. Shao, K. Sasaki, M. Vukmirovic, J. Zhang, N. Marinkovic, P. Liu, A. Frenkel, R. Adzic, *Nat. Mater.* **2009**, *8*, 325.
[11] H. Liang, H. Zhang, J. Hu, Y. Guo, L. Wan, C. Bai, *Angew. Chem. Int. Edt.* **2004**, *43*, 1540.
[12] H. Lee, S. Habas, S. Kweskin, D. Butcher, G. Somorjai, P. Yang, *Angew. Chem. Int. Edt.* **2006**, *45*, 7824.
[13] D. Xu, Z. Liu, H.Yang, Q. Liu, J. Zhang, J. Fang, S. Zou, K. Sun, *Angew. Chem. Int. Edt.* **2009**, *48*, 4217.
[14] C. Wang, H. Daimon, Y. Lee, J. Kim, S. Sun, *J. Am. Chem. Soc.* **2007**, *129*, 6974.
[15] J. Lu, I. Do, L. Drzal, R. Worden, I. Lee, *ACS Nano* **2008**, *2*, 1825.
[16] Y. Shao, S. Zhang, C. Wang, Z. Nie, J. Liu, Y. Wang, Y. Lin, *J. Power Sources* **2010**, *195*, 4600.
[17] C. Xu, X. Wang, J. Zhu, *J. Phys. Chem. C* **2008**, *112*, 19841.
[18] Y. Xin, J. Liu, Y. Zhou, W. Liu, J. Gao, Y. Xie, Y. Yin, Z. Zou, *J. Power Sources* **2011**, *196*, 1012.
[19] S. Park, Y. Shao, H. Wan, P. Rieke, V. Viswanathan, S. Towne, L. Saraf, J. Liu, Y. Lin, Y. Wang, *Electrochem. Commun.* **2011**, *13*, 258.
[20] D. Yu, L. Dai, *J. Phys. Chem. Lett.* **2010**, *1*, 467.
[21] W. Chen, S. Li, C. Chen, L. Yan, *Adv. Mater.* **2011**, *23*, 5679.
[22] Z. Tang, S. Shen, J. Zhuang, X. Wang, *Angew. Chem. Int. Ed.* **2010**, *49*, 4603.
[23] L. Qu, Y. Liu, J. Baek, L. Dai, *ACS Nano* **2010**, *4*, 1321.
[24] Y. Li, Y. Zhao, H. Cheng, Y. Hu, G. Shi, L. Dai, L. Qu, *J. Am. Chem. Soc.* **2012**, *134*, 15.
[25] S. Wang, D. Yu, L. Dai, D. Chang, J. Baek, *ACS Nano* **2011**, *5*, 6202.
[26] L. Yang, C. Hu, J. Wang, Z. Yang, Y. Guo, Z. Bai, K. Wang, *Chem. Commun.* **2011**, *47*, 8581.
[27] B. Lim, M. Jiang, P. Camargo, E. Cho, J. Tao, X. Lu, Y. Zhu, Y. Xia, *Science* **2009**, *324*, 1302.
[28] Z. Peng, H. Yang, *J. Am. Chem. Soc.* **2009**, *131*, 7542.
[29] L. Qu, L. Dai, *J. Am. Chem. Soc.* **2005**, *127*, 10806.
[30] L. Qu, L. Dai, E. Osawa, *J. Am. Chem. Soc.* **2006**, *128*, 5523.
[31] L. Jou, J. Chang, T. Twhang, I. Sun, *J. Electrochem. Soc.* **2009**, *156*, D193.
[32] Y. Xu, K. Sheng, C. Li, G. Shi, *ACS Nano* **2010**, *4*, 4324.
[33] W. Yang, S. Yang, W. Sun, G. Sun, Q. Xin, *Electrochim. Acta* **2006**, *52*, 9.
[34] Y. Wang, Y. Zhao, C. Xu, D. Zhao, M. Xu, Z. Su, H. Li, *J. Power Sources* **2010**, *195*, 6496.
[35] S. Hwang, S. Yoo, T. Jeon, K. Lee, T. Lim, Y. Sung, S. Kim, *Chem. Commun.* **2010**, *46*, 8401.
[36] H. Zhou, H. Wu, J. Shen, A. Yin, L. Sun, C. Yan, *J. Am. Chem. Soc.* **2010**, *132*, 4998.
[37] L. Wang, Y. Nemoto, Y. Yamauchi, *J. Am. Chem. Soc.* **2011**, *133*, 9674.
[38] C. Xu, H. Wang, P. Shen, S. Jiang, *Adv. Mater.* **2007**, *19*, 4256.
[39] Q. Wang, G. Sun, L. Jiang, Q. Xin, S. Sun, Y. Jiang, S. Chen, Z. Jusys, R. Behm, J. *Phys. Chem. Chem. Phys.* **2007**, *9*, 2686.
[40] F. Hu, C. Chen, Z. Wang, G. Wei, P. Shen, *Electrochim. Acta* **2006**, *52*, 1087.
[41] P. Ferreira, G. la O', Y. Shao-Horn, D. Morgan, R. Makharia, S. Kocha, H. Gasteiger, *J. Electrochem. Soc.* **2005**, *152*, A2256.
[42] C. Wang, D. van der Vliet, K. More, N. Zaluzec, S. Peng, S. Sun, H. Daimon, G. Wang, J. Greeley, J. Pearson, A. Paulikas, G. Karapetrov, D. Strmcnik, N. Markovic, V. Stamenkovic, *Nano Lett.* **2011**, *11*, 919.